A Frequency Domain Approach to the Recovery of Geophysical Potentials

Michael Rauth and Thomas Strohmer

Abstract— **A major difficulty in the recovery of geophysical potentials arises from the fact that the available data are in general noisy and irregularly spaced. Analysis and further processing require a representation of the potential field on a regular grid. An analysis of the Fourier transform of potential fields suggests an approximation by band-limited functions. We show that the resulting discrete least squares problem can be formulated as a linear system of equations, where the system matrix is of block-Toeplitz type. The properties of potential fields in the frequency domain together with the special structure of the system matrix lead to a robust and computationally attractive solution via the Fast Fourier transform and the conjugate gradient algorithm. We show how additional knowledge about the statistics of the data can be incorporated in our algorithm. Experimental results for synthetic gravity data demonstrate good performance for irregularly spaced noisy sampling sets.**

I. Introduction

The essential aim of exploration geophysics is to detect and analyze geological subsurface structures associated with oil, gas, and other raw materials. One way of doing this is to study anomalies of the potential fields, i.e. the gravity and magnetic field, as they are the manifestation of differences in the physical properties, giving a clue to the type and distribution of different minerals in the region of interest.

A wide variety of numerical procedures, including map-drawing algorithms and Fourier analysis, require the data on a regularly spaced lattice. In contrast, most geophysical data are acquired at individual observation points or along profiles. Thus sampling points are irregularly spaced (scattered) [1].

It is therefore necessary to construct an representation of the potential, or the underlying function in general, on a grid, given observations of the value of the function at arbitrary locations in space. This operation is called gridding. A variety of gridding algorithms can be found in the literature. For an overview see e.g. [2] and the references given there. For potential field data, there is no unique mathematically preferred gridding algorithm, because the data for a potential field on a 2-D surface can be specified freely.

Nevertheless for the evaluation of a gridding algorithm one has to consider the following aspects: The first involves the global properties of the solution. If a priori information about the solution, like the nature of the underlying physical process or its functional form in general, is known the algorithm should construct a solution of the appropriate type. The second aspect deals with constrains given by the data, e.g. data contaminated by noise, which is not necessarily of the same magnitude for subsets of the samples, should be approximated within the error envelope rather than exactly interpolated. The third aspect involves the method of interpolation or approximation in regions of sparse control, where the result should not exhibit features not apparently controlled by the observations. The solution of gridding algorithms differs most in these sparsely sampled regions and appropriate global properties can lead to an improvement. Furthermore there are practical aspects such as computational efficiency in terms of speed and memory storage.

Existing algorithms cover some of these aspects but not all of them. Based on a frequency domain approach we develop a gridding method that exploits the knowledge about the global shape of geophysical potentials in the Fourier domain, and is subject to all the aspects mentioned above.

The paper is divided into a theoretical and an experimental part. In the first part we summarize the properties of the gravity and magnetic field and give expressions for their representation in the Fourier domain. It is demonstrated how the behavior of the spectrum of geophysical potentials suggests an approximation by trigonometric polynomials. We then present the algorithm and give details about a numerical implementation. In the second part we give a numerical example to study the performance of the method.

II. Theory

We first give expressions for the gravity and the magnetic field in the Fourier domain and demonstrate that they are so-called essentially band-limited functions. Since functions of that type can be well approximated by strictly band-limited functions, we can use methods originally developed for the irregular sampling problem of band-limited functions, to design an efficient algorithm for the approximation of the gravity and the magnetic field.

For a precise description of the problem, suppose that we have a set of r distinct irregularly distributed sampling points $\mathbf{x}_j = (x_1, x_2)$ in an interval, say $[0, N) \times [0, N)$, and sampling values $s_j = f(\mathbf{x}_j) + \epsilon_j$, where f is the underlying potential function and ϵ_j the error arising from imperfect measurements or preprocessing. Since we are developing a 2-D method, we implicitly assume all sampling points at a constant altitude x_3.

The task is to find a reasonable and computable approximation of f on a finite and discrete set of regularly spaced grid points $\mathbf{\Delta} = \{(\Delta_1, \Delta_2)\}$ for $\Delta_j = 0, \ldots, N-1$. Choosing the interval of regular grid points as square is no loss of generality, since all other intervals can be obtained by

Michael Rauth is with the Department of Geophysics, University of Vienna, Nordbergstr.17, A-1090 Wien, Austria. E-mail: rauth@tyche.mat.univie.ac.at

Thomas Strohmer is with the Department of Mathematics, University of Vienna, Strudlhofg.4, A-1090 Wien, Austria. E-mail: strohmer@tyche.mat.univie.ac.at

simple rescaling.

A. Potential fields in the Fourier domain

Let $\hat{f}$ denote the continuous 2D-Fourier transform of the function f defined by

$$\hat{f} = \int_{-\infty}^{\infty} f e^{-i\mathbf{v}\cdot\mathbf{x}} d\mathbf{x}, \tag{1}$$

where $\mathbf{x} = (x_1, x_2)$ and $\mathbf{v} = (v_1, v_2)$ are the spatial and the angular frequency coordinates respectively, $\mathbf{v}\cdot\mathbf{x} = v_1x_1 + v_2x_2$, and i denotes the imaginary unit. Further we write $\mathbf{v}^*$ for the conjugate transpose, and $\|\mathbf{v}\|$ for the l^2-norm of $\mathbf{v}$.

From potential theory it is well known that the continuous Fourier transform of a gravitational potential U caused by a density distribution $\rho(\xi_k)$ at a point (x_k), $k = 1, 2, 3$, above the distribution is given by [3], [4], [5]

$$\hat{U} = 2\pi G \int_{-\infty}^{x_3} \frac{\hat{\rho}}{\|\mathbf{v}\|} e^{-(x_3-\xi_3)\|\mathbf{v}\|} d\xi_3, \tag{2}$$

where G is the gravitational constant and x_3 is positive upwards.

In practice one usually measures the vertical component of the gravitational acceleration g_3. Its representation in the frequency domain can be derived by differentiating equation (2) with respect to ξ_3:

$$\hat{g}_3 = 2\pi G \int_{-\infty}^{x_3} \hat{\rho}\, e^{-(x_3-\xi_3)\|\mathbf{v}\|} d\xi_3. \tag{3}$$

Similar expressions hold for the magnetic potential V: Let $m(\xi_k)$ be a magnetic distribution. Let L_k and l_k be the direction cosines of the direction of magnetization and of the component being measured respectively. Introducing the abbreviations

$$\begin{aligned} \bar{L} &= iL_1v_1 + iL_2v_2 + L_3\|\mathbf{v}\| \\ \bar{l} &= il_1v_1 + il_2v_2 + l_3\|\mathbf{v}\| \end{aligned}$$

the potential $\hat{V}$ and the field intensity $\hat{M}$ in the frequency domain write as

$$\hat{V} = 2\pi\bar{L} \int_{-\infty}^{x_3} \frac{\hat{m}}{\|\mathbf{v}\|} e^{-(x_3-\xi_3)\|\mathbf{v}\|} d\xi_3 \tag{4}$$

and

$$\hat{M} = 2\pi\bar{L}\,\bar{l} \int_{-\infty}^{x_3} \frac{\hat{m}}{\|\mathbf{v}\|} e^{-(x_3-\xi_3)\|\mathbf{v}\|} d\xi_3. \tag{5}$$

With the assumption that the sources $\rho(\xi_k)$ and $m(\xi_k)$ are restricted to a localized region below the plane of measurement, i.e. $x_3 > \xi_3$, it follows that the integrals in equations (3) and (5) exist and are also finite.

Thus we can conclude that the magnitude of the spectrum of the gravity and the magnetic field decay exponentially with increasing frequency index $\mathbf{v}$. In other words, the contribution of high frequencies is negligible in some sense. Functions with this property belong to a larger class, the so-called essentially band-limited functions. We define the space of 2-D *essentially Ω-band-limited* functions $\mathcal{B}_{\Omega,\delta}$ by

$$\mathcal{B}_{\Omega,\delta} = \left\{ f : \int_{\mathbf{v}>\Omega} |\hat{f}(\mathbf{v})|^2 d\mathbf{v} \le \delta^2 \|f\|^2 \right\}, \tag{6}$$

where δ is a small number. A function is called strictly Ω-band-limited (or simply band-limited) if $\delta = 0$.

It is well-known that a band-limited function can be reconstructed from its (uniformly or non-uniformly spaced) sampling values, if the sampling points satisfy some density criterion [6], [7]. If f is an essentially band-limited function, it cannot be completely reconstructed from its sampling values. If we compute f nevertheless from its samples we commit an error, the so-called *aliasing error*. An estimate for the error of approximating essentially band-limited functions by strictly band-limited functions will be given in equation (16).

B. Potential fields and trigonometric polynomials

The analysis of the discrete nonuniform sampling problem of band-limited functions suggests an approximation of a continuous band-limited function by *trigonometric polynomials* [8], [9].

Thus for any integer $M > 0$ we consider the $(2M+1)^2$-dimensional space $\mathcal{P}_M$ of 2-D trigonometric polynomials of degree M^2

$$p(\mathbf{x}) = \sum_{\mathbf{v}=-M}^{M} c_{\mathbf{v}} e^{2\pi i \mathbf{v}\cdot\mathbf{x}/N^2} \tag{7}$$

where the coefficients c uniquely determine p. For simplicity of representation we assume that p has the same number of coefficients in both frequency coordinates. Clearly all results in this paper hold for trigonometric polynomials with a different number of coefficients in the frequency coordinates. To avoid unnecessary introduction of new variables we slightly abuse our notation by treating the $(2M+1) \times (2M+1)$ array c also as a vector by stacking the columns of c.

We look for a trigonometric polynomial $p \in \mathcal{P}_M$ with $(2M+1)^2 \le r$ that approximates the potential f at the user-defined set $\mathbf{\Delta}$ of regularly spaced grid points.

In order to find the optimal trigonometric polynomial $\tilde{p}$ for a given M we consider the following least squares problem: Given the samples as defined above, weights $w_j > 0$, and the degree of the polynomial, we want to find a polynomial $\tilde{p}$ that solves

$$\min \sum_{j=1}^{r} |s_j - p(\mathbf{x}_j)|^2 w_j \tag{8}$$

where the minimum is taken over all trigonometric polynomials $p \in \mathcal{P}_M$.

Introducing the weights w_j in equation (8) allows to incorporate information about varying quality of the measurements s_j. This information can be included in a straightforward way, by assigning smaller weights to less precise and larger weights to more accurate measurements.

The second-named author has shown that the coefficients $\tilde{c}$ of the polynomial $\tilde{p}$ can be computed by solving the linear system of equations $T\tilde{c} = b$ (cf. [10]), and its solution $\tilde{c}$ can be found by minimizing $\|Tc - b\|$. Details about T and b will be given in the next section.

However the fact that $\tilde{p}$ is the optimal solution of (8) for a fixed M does not necessarily imply that $\tilde{p}$ is also the optimal solution for $\min \|f - p\|$ or $\min \|f(\mathbf{\Delta}) - p(\mathbf{\Delta})\|$, especially since the samples s_j are in general contaminated

by noise. Clearly we cannot compute the optimal solution of $\min \|f(\mathbf{\Delta}) - p(\mathbf{\Delta})\|$ for a given M, but we can improve our approximation $\tilde{p}$ by using our knowledge about the original function f being a potential field. This can be done in the following way:

We look for a polynomial $\bar{p}$ which is close to the minimum $\tilde{p}$ in the sense that

$$\sum_{j=1}^{r} |s_j - \bar{p}(\mathbf{x}_j)|^2 w_j \approx \sum_{j=1}^{r} |s_j - \tilde{p}(\mathbf{x}_j)|^2 w_j,$$

but we do not force $\bar{p}$ to be the optimal solution of (8).

Instead we make use of the knowledge that our data arose from geophysical potentials to compute $\bar{p}$. We therefore require the frequency components of $\bar{p}$, which are nothing else than the coefficients $\bar{c}$ in equation (7), to resembles the shape of potential field spectra.

A simple but efficient technique to incorporate the a priori knowledge about the solution is the following: Instead of using the standard l^2 norm $\|.\|$, we introduce a weighted l^2 norm $\|.\|_d$ by

$$\|z\|_d^2 = \sum_{\mathbf{k}=-M}^{M} |z_{\mathbf{k}}|^2 d_{\mathbf{k}}^2 . \tag{9}$$

From equations (3) and (5) we know that potential fields show an exponential decay in their frequency components, so the appropriate choice for the frequency weights is

$$d_{\mathbf{k}} = e^{-\|\mathbf{k}\|} . \tag{10}$$

Treating d as vector by stacking its columns, leads to the definition of the diagonal matrix D by $D = \mathrm{diag}(d)$. Since

$$\min_c \|Tc - b\|_d = \min_c \|DTc - Db\|,$$

we compute the polynomial $\bar{p}$ whose coefficients $\bar{c}$ solve

$$\min \|DTc - Db\| , \tag{11}$$

and resemble the spectrum of a potential field.

C. Efficient approximation of potential fields

In this section we present a fast and stable algorithm for solving (11), which is essentially based on the so-called ACT method proposed in Feichtinger et al. [9]. It is crucial for the proposed algorithm that T is a *block Toeplitz matrix*, i.e. T is of the form

$$T = \begin{bmatrix} B_0 & B_1 & \cdots & B_{N-1} \\ B_{-1} & B_0 & \cdots & B_{N-2} \\ \vdots & \vdots & & \vdots \\ B_{-N+1} & B_{-N+2} & \cdots & B_0 \end{bmatrix} \tag{12}$$

where each B_i itself is a Toeplitz matrix, i.e. the entries of B_i are constant down each diagonal.

An important advantage of linear systems of equations with Toeplitz or block Toeplitz matrices is that their solution can be found with considerably less computational effort than general systems of equations [11], [12]. The *conjugate gradient method* (CG) is known as an efficient iterative method to solve linear systems of equations [13] and it is particularly well suited for Toeplitz-like systems [12]. A detailed discussion of CG can be found for instance in Golub and van Loan [14].

Since all entries of the diagonal matrix D are strictly positive, the matrix D itself is positive definite and symmetric. Thus formally the use of a weighted norm via applying D resembles the the application of a preconditioner but has a completely different interpretation in this context: We do neither expect that DT has a lower condition number than T nor that DT has better clustered eigenvalues. However we can directly apply the formulas for the *preconditioned conjugate gradient method* (PCG) to solve (11).

In the sequel we present our algorithm for the reconstruction of a potential field f from scattered data:

Algorithm 1:

Input: Sampling points $\mathbf{x_j}$, the sampling values s_j, the weights w_j, $j = 1, \ldots, r$, the accuracy threshold tol, and the degree M^2 of the polynomial, such that $r \geq (2M+1)^2$.

Step 1: Compute the entries of T and b by

$$T_{\mathbf{vu}} = \sum_{j=1}^{r} w_j e^{2\pi i(\mathbf{v}-\mathbf{u})\cdot\mathbf{x}_j/N^2} \tag{13}$$

$$b_{\mathbf{v}} = \sum_{j=1}^{r} w_j s_j e^{2\pi i \mathbf{v}\cdot\mathbf{x}_j/N^2} \tag{14}$$

for $|v_1|, |v_2|, |u_1|, |u_2| \leq M$.

Step 2: Initialize $r_0 = b, c_0 = 0, n = 0$ and compute $\bar{c}$ iteratively:

while *accurate* $> tol$
  $z_n = Dr_n$
  $n = n + 1$
  if $n = 1$
    $q_1 = z_0$
  else
    $\beta_n = r_{n-1}^* z_{n-1} / r_{n-2}^* z_{n-2}$
    $q_n = z_{n-1} + \beta_n q_{n-1}$
  end
  $\alpha_n = r_{n-1}^* z_{n-1} / q_n^* T q_n$
  $c_n = c_{n-1} + \alpha_n q_n$
  $r_n = r_{n-1} - \alpha_n T q_n$
end
$c_* = c_n$

Step 3: The solution $\bar{p}$ is then given by

$$\bar{p}(\mathbf{x}) = \sum_{\mathbf{v}=-M}^{M} \bar{c}_{\mathbf{v}} e^{2\pi i \mathbf{v}\cdot\mathbf{x}/N^2} \tag{15}$$

for $v_1, v_2 = 0, \ldots, N-1$.

Several choices for the stopping procedure *accurate* can be found in the literature [13]. Since we want to fit the error envelope of the data, a suitable criterion for our situation is to stop the iterations as soon as the error of the approximation at the sampling points becomes smaller than the measurement error.

Lemma 1: The aliasing error for approximating a potential field f from its samples $f(\mathbf{x}_j)$ on a regular grid $\mathbf{\Delta}$ by Algorithm 1 can be estimated by

$$\|f(\mathbf{\Delta}) - \tilde{p}(\mathbf{\Delta})\| \leq \sqrt{\delta(1 + \lambda^{-1})} \|f(\mathbf{\Delta})\| \tag{16}$$

where λ is the minimal eigenvalue of the matrix T, and δ is defined by equation (6).

The proof is given in [10].

Often the bandwidth of the signal to recover is unknown. Thus we have to estimate the bandwidth from nonuniformly spaced noisy samples. This question can be seen

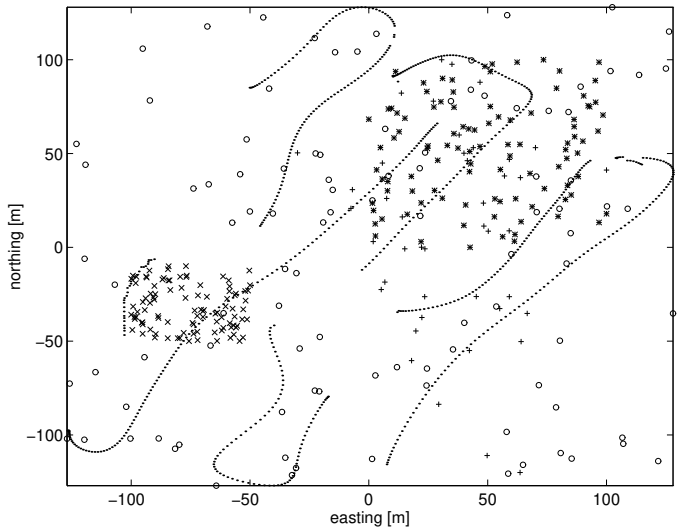

Fig. 1. The sampling geometry for the test examples. The 1000 sampling points belong to 5 subsets, namely line type data (657 points, indicated by dots, S1), a random part (100 points, small circles, S2), a dense cluster (100 points, 'x', S3), a not so dense cluster (100 points, '∗', S4), and a rather sparse cluster (43 points, '+', S5).

as a regularization problem, which however cannot be attacked by standard regularization techniques. A multiscale method to solve for the optimal bandwidth in presence of noise will be presented in a forthcoming joint paper of O. Scherzer and the second author [15].

D. Complexity of the algorithm

Due to the block-Toeplitz structure the whole information of T is stored in the first and M-th column of T. Hence the computational effort for the calculation of the relevant entries of T and b in Step 1 is of order $\mathcal{O}(rM^2)$ operations. Recently a fast algorithm has been proposed for the approximative evaluation of trigonometric sums of the form (13) and (14) [16]. This algorithm allows to reduce the computational complexity of Step 1 to $\mathcal{O}(M^2 \log M + r(\log 1/\varepsilon)^2)$, where ε is the precision for computing T and b.

The main effort in Step 2 is one matrix-vector multiplication in each iteration. It is essential for the efficiency in terms of speed and memory of the proposed algorithm that multiplication of a vector by the block-Toeplitz matrix T can be computed using 2-D FFT, analogous to Toeplitz matrices [12]. Thus the computational effort of Step 2 is $\mathcal{O}(\kappa M^2 \log M)$ operations where κ is the number of iterations.

Equation (15) in Step 3 can be evaluated in $\mathcal{O}(N^2 \log N)$ operations by defining $\bar{c}\mathbf{v} = 0$ for $M+1 \le |v_1|, |v_2| \le N/2$ and replacing (15) by

$$\bar{p}(\mathbf{x}) = \sum_{\mathbf{v}=-N/2}^{N/2-1} \bar{c}\mathbf{v} e^{2\pi i \mathbf{v}\cdot\mathbf{x}/N^2}. \tag{17}$$

Equation (17) can be computed by a 2-D FFT for an appropriate choice of N.

Since trigonometric polynomials are periodic functions our approximation is periodic at the boundaries. A potential field is in general not periodic. Thus our reconstruction will show some artifacts at the boundaries. However these artifacts can be kept small, by choosing the regular grid $\mathbf{\Delta}$ somewhat larger than suggested by the data and reducing the resulting approximation to the original region of interest.

III. Experimental results

In this section we study the performance of the proposed method by reconstructing a synthetic gravitational anomaly which represents the gravitational acceleration due to an ensemble of buried rectangular boxes of different size, depth and density contrast. The original anomaly is depicted in Figure 2a.

This anomaly was then sampled at a highly irregularly distributed set of 1000 sampling points. The sampling geometry is depicted in Figure 1. Note that this set consists of 5 components: line type data (657 points, S1), which is characteristic for airborne or other fast moving measuring devices, a random part (100 points, S2), a dense cluster (100 points, S3), a not so dense cluster (100 points, S4), and a rather sparse cluster (43 points, S5). Thus there is a severe anisotropy in the spatial data density. We choose this sampling set since it shows all features which are typical for real-world settings[1].

We then reconstructed the anomaly from the samples on a grid of the size 256×256 and a spacing of 1m. To measure the quality of the approximation, the relative deviation of the reconstructed anomaly from the original one evaluated at the grid points in percent has been calculated via

$$\frac{\|\bar{p}(\mathbf{\Delta}) - f(\mathbf{\Delta})\|}{\|f(\mathbf{\Delta})\|} \cdot 100. \tag{18}$$

In a first experiment we study the performance and robustness of Algorithm 1 and compare it to the standard ACT method. A second experiment will treat the influence of noise of different magnitude in all subsets.

A. Experiment 1: The performance of Algorithm 1

As real world measurements have always a certain amount of error, we added white noise with an amount of 1% to 20% of the energy $\|s\|$ of the sampling set to our data. In this first experiment all data were of the same accuracy, thus we did not use statistical weights, which is equivalent to assigning the sample s_j a weight $w_j = 1$.

In order to study the gain in performance by our frequency domain approach compared to the standard ACT algorithm, we calculated the solution to our problem with and without weights in the Fourier domain. The dependence of the approximation error at the grid points and at the samples as a function of the amount of noise together with the degree of the polynomial and the number of iterations for both cases is given in Table I.

As an example the approximation of the potential field from the data with 2% noise by the standard ACT method and Algorithm 1 are depicted in Figure 2b and Figure 2c respectively. The importance of incorporating the knowledge about the shape of the spectrum becomes clear if we regard the error at the grid points. For the approximation by ACT the mean error is 0.149 ± 0.195mGal, the maximum being 1.281mGal. For Algorithm 1 we have a mean

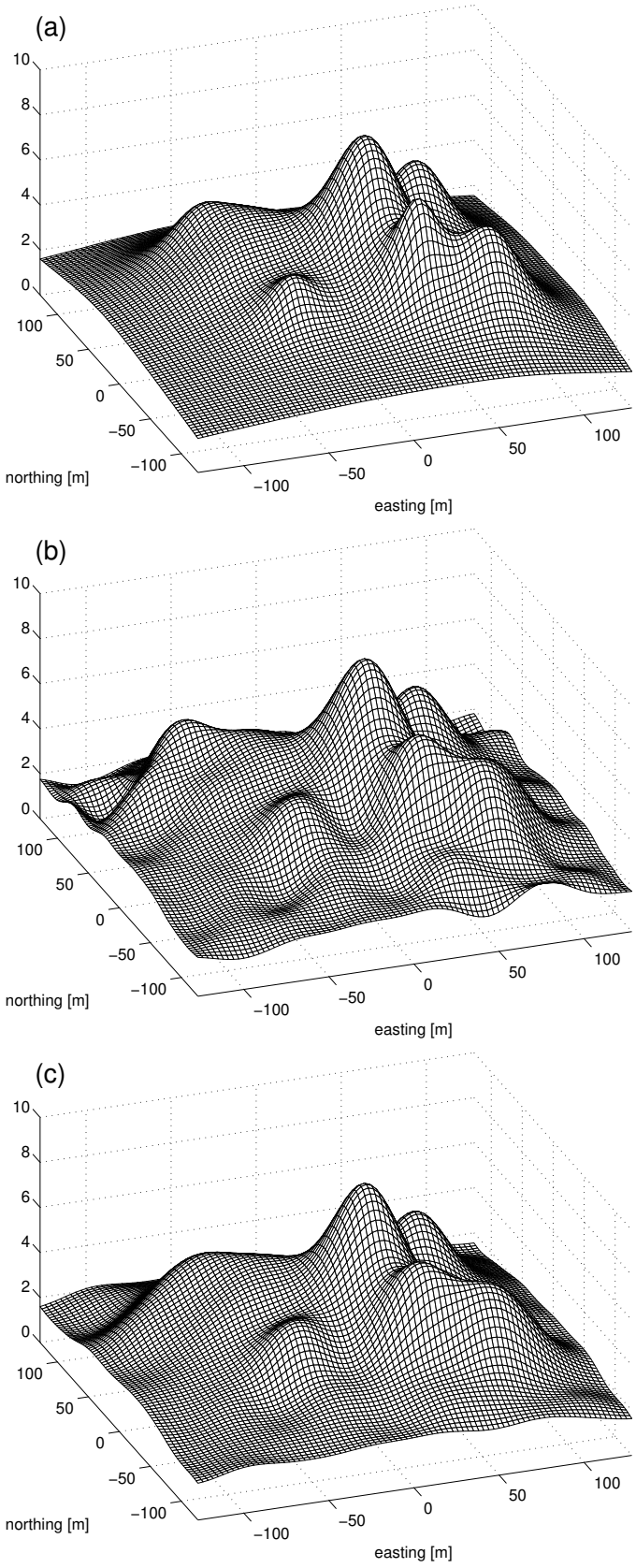

Fig. 2. (a) The original synthetic gravity anomaly, (b) approximation of the original anomaly from the samples after adding 2% of white noise by the standard ACT algorithm, (c) approximation by Algorithm 1. The gravitational acceleration is given in mGal

TABLE I

Approximation error as function of noise

Noise in %	Error of ACT in % Deg.	Iter.	grid	samples	Error of Algorithm 1 in % Deg.	Iter.	grid	samples
0	225	961	6.75	10^{-3}	225	463	2.45	0.49
1	49	200	7.26	1.00	225	418	2.97	1.06
2	36	146	6.49	2.00	225	420	3.44	2.00
5	25	106	6.76	5.00	144	304	4.91	4.99
10	25	97	9.43	9.96	100	208	7.02	9.99
20	16	61	11.53	19.94	64	140	9.57	20.00

error of 0.086 ± 0.097mGal, and the maximal deviation is 0.791mGal. We see that the mean error is much smaller for our algorithm. Moreover it is only slightly bigger than the standard deviation of the error, being 0.079mGal in this case. This is a satisfying result, as we reconstructed from noisy samples that did not cover all details of the original anomaly.

Comparing the approximations with the original anomaly visually we make the following observations: Both functions look very similar in the central part of the area, and all important features are well represented. The appearance of the approximation with weights (Fig. 2c) is of a smoothness comparable to that of the original anomaly (Fig. 2a), and smoother than the approximation without weights (Fig. 2b), and any interpolation of the noisy data would be.

The main difference between the original function and the approximations is on the boundary of the region, where the latter show some spurious features. These are caused by the periodicity of the approximation, as mentioned above.

If we compare the approximation by the ACT method and Algorithm 1 we see that boundary effects are much more pronounced for the former. Moreover it becomes obvious that the maximal error occurs in regions of sparse control. The approximations by ACT exhibits features not apparently controlled by the observations, whereas the solution computed with our Algorithm does not show this behavior. Our Fourier domain approach yields the biggest gain in performance in these sparsely controlled regions as it honors the global properties of potential fields.

As much as the behavior of the approximation error as a function of noise is concerned (Table I), it is clear that also in the absence of noise there is an intrinsic error. This is due to the fact that not all features are sampled and we approximate an essentially band-limited function by a really band-limited one. Again the use of frequency weights leads to a strong improvement of the quality of the approximation.

Approximation by the standard ACT algorithm is excellent at the sampling points but the deviation from the true anomaly as evaluated on the grid points is rather unsatisfying. Only for a big amount of noise the results become better, which is basically due to the properties of the CG-method.

Considering the approximation by Algorithm 1, we see that the result is much more satisfying. The error increases

TABLE II
Approximation error and statistical weights

Noise in % Subset						Error without weights				Error with weights			
								grid	samples			grid	samples
S1	S2	S3	S4	S5	total	Deg.	Iter.	%	%	Deg.	Iter.	%	%
1	2	5	10	20	7.01	81	176	5.34	7.00	121	225	4.64	7.01
20	1	2	5	10	16.21	81	154	7.43	16.21	81	192	4.63	16.21
10	20	1	2	5	10.10	64	142	11.27	10.10	81	143	9.18	10.08
5	10	20	1	2	7.18	121	216	7.25	7.18	144	251	6.30	7.18
2	5	10	20	1	8.04	81	196	5.91	8.04	100	222	5.04	8.04

linearly with increasing noise, until a point is reached where the noise is of the same magnitude as the periodicity error, and the method performs better and better. The global error augments then only to the proportion of small scale features which get lost in the noise level. Note that even for the case of 20% noise in the samples the global error is still only 9.6%. The computational expenses decrease with increasing noise.

B. Experiment 2: Data of varying quality

In geophysical practice it is not uncommon to have data of different quality. This might result from measuring with different devices or under changing conditions, e.g. background noise. In order to simulate such a case we added different amount of noise to the five components S1,. . . ,S5 of our sampling set (Fig. 1). We then calculated an approximation on the same grid as for the first experiment with Algorithm 1. First we did not incorporate our knowledge about the various levels of noise, and assigned each sample s_j a weight $w_j = 1$. In a second run we exploited this valuable information by assigning each sample s_j a weight inverse proportional to its amount of noise in percent, i.e. $w_j = 1/n, n = 1, 2, 5, 10, 20$. The experiment was repeated for all permutations of noise and sampling sets. Table (II) lists the varying amounts of noise, the resulting overall noise, and shows the approximation error together with the degree of the polynomial and the number of iterations. It becomes obvious that incorporating all available information lead to a better result in all five cases. The price one has to pay are higher computational costs, as the use of statistical weights increases the degree of the approximating polynomial and the number of iterations.

IV. Conclusion

The gridding method proposed in this paper shows a good performance for the approximation of potential field data from highly irregular sampling sets under the presence of noise. It is maybe one of the first methods which addresses extremely anisotropic geometries, like line-type data, incorporates the physical background of the process being measured, and has the capability to include statistical information, such as varying data quality, by easy means. Furthermore the algorithm is in some sense of minimum complexity from a computational point of view, as it depends mainly on the number of samples and the size of the spectrum. The price of has to pay is the periodicity of the solution, which may lead to unwanted boundary effects.

We believe that our method is of strong practical relevance in the situations described above but it is still the scientist who has to select the appropriate method to grid his data, depending on the actual geometry of the sampling set, the quality of the data and the resources available for processing.

V. Acknowledgments

The authors have been supported by the projects P10473-GEO and S7001-MAT of the Austrian Science Foundation FWF respectively.

References

[1] M. Rauth. Application of 2-D methods for scattered data approximation to geophysical data sets. In *Sampling in Theory and Applications*, pages 38–43, Jurmala, Latvia, 1995.

[2] T.A. Foley and H. Hagen. Advances in scattered data interpolation. *Surv. Math. Ind.*, 4:71–84, 1994.

[3] B.K. Bhattacharyya. Continous spectrum of the total-magnetic-field anomaly due to a rectangular prismatic body. *Geophysics*, 31(1):97–121, 1966.

[4] P.J. Gunn. Linear transformations of gravity and magnetic field. *Geophysical Prospecting*, 23:300–312, 1975.

[5] R.J. Blakely. *Potential theory in gravity and magnetic applications*. Cambridge University Press, 1995.

[6] H.G. Feichtinger and K.H. Gröchenig. Theory and practice of irregular sampling. In J. Benedetto and M. Frazier, editors, *Wavelets: Mathematics and Applications*, pages 305–363. CRC Press, 1994.

[7] J.R. Higgins. *Sampling Theory in Fourier and Signal Analysis: Foundations*. Oxford University Press, 1996.

[8] K. Gröchenig. Irregular sampling, Toeplitz matrices, and the approximation of entire functions of exponential type, 1994. Preprint.

[9] H. G. Feichtinger, K. Gröchenig, and T. Strohmer. Efficient numerical methods in non-uniform sampling theory. *Numerische Mathematik*, 69:423–440, 1995.

[10] T. Strohmer. Computationally attractive reconstruction of band-limited images from irregular samples. *IEEE Trans. on Image Processing, to appear*, 6(4):540–548, 1997.

[11] G. Ammar and W. Gragg. Superfast solution of real positive definite Toeplitz systems. *SIAM J. Matrix Anal. Appl.*, 9:61–76, 1988.

[12] R.H. Chan and G. Strang. Toeplitz equations by conjugate gradients with circulant preconditioner. *SIAM J. Sci. Stat. Comput.*, 10:104–119, 1989.

[13] L.A. Hageman and D.M. Young. *Applied Iterative Methods*. Academic Press, 1981.

[14] G.H. Golub and C.F. van Loan. *Matrix Computations, third ed.* Johns Hopkins, London, Baltimore, 1996.

[15] O. Scherzer and T. Strohmer. A multi–level algorithm for the solution of moment problems. preprint, 1997.

[16] G. Beylkin. On the fast Fourier transform of functions with singularities. *Appl. Comp. Harm. Anal.*, 2(4):363–381, 1995.